MULTI−TAPER COHERENCE RECEIVER FUNCTIONS AND P−WAVE SCATTERING WITHIN THE CRUST AND LITHOSPHERE: THE VIEW FROM ARABIA

Jeffrey Park, Vadim Levin
Department of Geology and Geophysics, Yale University

Sponsored by U. S. Department of Defense
Defense Threat Reduction Agency
Arms Control Technology Center
Contract No. DSWA01−98−011

ABSTRACT

We apply a new receiver function (RF) inversion technique that uses multi−taper coherence estimates instead of spectral division. The multi−taper spectrum estimates are leakage resistant, so that low−amplitude portions of the *P*−wave spectrum can contribute usefully to the RF estimate. The coherence between vertical and horizontal components can be used to obtain a frequency−dependent uncertainty for the RF, which is very useful for weighting RF stacks.

Teleseismic RFs for Global Seismographic Network station RAYN on the eastern edge of the Arabian Shield contain a strong converted−phase P_Hs that we believe arises from the Hales discontinuity at the depth of ~70 km. The RAYN RFs also indicate that a similar zone borders the crust−mantle transition at ~40km. Synthetic seismograms computed in simple one−dimensional anisotropic models help us explore the range of scenarios that would match observed receiver functions. The RFs require, assuming hexagonal anisotropy, a tilted symmetry axis with a north−south strike. In our preferred model the anisotropic zones are bounded by sharp discontinuities at the top and by smooth gradients below. The gradients extend downward from the Moho and the Hales discontinuities. Within both anisotropic zones the symmetry axes, indicative of fabric in the olivine−dominated upper mantle rock, are oriented along the N−S direction (±10°), and are tilted 50° toward the south. We propose that these regions of coherent fabric within the upper mantle represent the development of shear zones during the late Proterozoic continent−continent collision, when the the Ar−Rayn tectonic block was involved in an episode of northward "escape" along the northern flank of the Najd fault system.

P waves from regional−distance earthquakes are complex and reverberatory, as would be expected from a combination of head waves, post−critical crustal reflections and shallow−incident *P* from the upper mantle. Nevertheless, regional−distance RFs for GSN stations RAYN and ANTO show some agreement with teleseismic RFs. At RAYN the moveout of the Moho−converted Ps phase, relative to direct P, follows well the predictions of the IASP91 earth model. The Moho−converted Ps phase shows complexity associated with the transition−zone triplication near Δ=20° and constant delay (zero moveout) as Δ−−>0, consistent with conversion from P_n. Similar behavior is seen at ANTO for events that arrive from the west. For eastern backazimuths the ANTO RFs show features whose moveout is negative as Δ−−>0. This moveout is poorly fit by reverberations in flat layers or by direct scattering from a dipping interface, but is consistent with a topographic scatterer a few 10s of km eastward of the ANTO site. Regional receiver functions may therefore be useful in judging whether teleseismic RFs at a particular station are suitable candidates for a 1−D velocity structure inversion. Synthetic seismograms of regional *P* phases, computed with a locked−mode reflectivity approach, confirm many of the observed features of the RAYN and ANTO regional receiver functions.

Key Words:

P waves, receiver function, Arabian Shield, continental lithosphere, seismic anisotropy, scattered waves, regional seismic wave propagation

OBJECTIVE

Proper detection and discrimination of seismic waves from suspected clandestine explosions is best accomplished when the wave−propagation characteristics of the Earth between the source and the seismometer are well−known. Teleseismic body waves from earthquakes and explosive sources experience scattering as they travel upwards through the uppermost mantle and crust. Regional body waves experience scattering as they travel through the crustal waveguide. The objective of this research project is to use variations in the elastic anisotropy of the crust and uppermost mantle to describe the scattering that is observed in seismic data. Many models for seismic scattering invoke a statistical 3−D distribution of small−scale anomalies in isotropic *P* and *S* seismic velocities e.g., the phase−screen approach (Wu, 1994) or finite−difference computations (e.g. Levander and Hollinger, 1992). The motivation for using anisotropy is threefold. First, fairly modest fluctuations in anisotropic properties can cause significant conversion of *P* (compressional) motion to *S* (shear) motion in propagating seismic waves. Second, numerical experiments have shown that flat−layered anisotropic media can cause large scattered wavetrains in both surface waves (Park, 1996) and body waves (Levin and Park, 1997; 1998; Savage, 1998). Third, elastic anisotropy, as a material property of rocks, seems to be the rule rather than the exception, caused by aligned cracks (Hudson, 1981), by lattice−preferred mineral orientation within rocks (Babuska and Cara, 1991), and by fine−layering (Helbig, 1994). Large−scale 3−D velocity structures are not necessary to create a P−coda or an extended surface−wave signal, at least in theory. If a 1−D anisotropic seismic−velocity structure can usefully represent much of the scattered seismic energy in an incoming signal at a particular seismic observatory, there are practical benefits. An analyst, faced with a complex seismic signal to interpret, would likely need to know fewer parameters of earth structure local to the station, and may run simpler synthetic seismogram codes to reproduce the data.

Although this research focusses on developing anisotropic models for crustal seismic velocities, the receiver functions themselves are useful in the verification and monitoring of a Comprehensive Nuclear−Test−Ban Treaty (CTBT). Receiver functions represent empirically the scattering of compressional (*P*−wave) to shear (*S*−wave) energy at particular seismic stations. Since explosions radiate an surfeit of P−wave energy relative to earthquakes, the conversion of *P* to *S* energy makes the discrimination problem more difficult. Receiver functions can be useful empirically if they explain a significant fraction of scattering in seismic records, even if no simple earth−structure model can explain them.

RESEARCH ACCOMPLISHED

A key objective of this research is to determine whether layered anisotropy is pervasive in the crust and has a strong influence on body−wave coda. Computational modeling (Cassidy, 1992; Kosarev et al 1994; Levin and Park, 1997; 1998; Savage, 1998) demonstrates that both anisotropy and dipping interfaces cause predictable variations in *P*−to−*S* scattered energy, dependent on the incoming direction of the *P*−wave −− its angle of incidence (or equivalently, its slowness *p*), and its back−azimuth angle ϕ. The *P*−to−*SH* energy scattered to the transverse−horizontal component of motion is particularly diagnostic, as its amplitude is predicted to reverse from positive to negative, and vice versa, in a lobate pattern with back−azimuth ϕ. We have analysed seismic data from several permanent seismic observatories to study the back−azimuth dependence of receiver functions.

Receiver Functions From Multiple−Taper Spectral Correlation Estimates.

The simplest way to estimate a receiver function (RF) is by spectral division, a ratio of Fourier transforms for the different components: $H_R(f) = Y_R(f)/Y_Z(f)$ and $H_T(f) = Y_T(f)/Y_Z(f)$. Here $Y_Z(f)$, $Y_R(f)$, and $Y_T(f)$ are the Fourier spectra of the vertical, radial and transverse seismic components, respectively. An inverse Fourier transform converts spectral−domain receiver functions $H_R(f)$ and $H_T(f)$ into a prediction filter of *Ps* scattered waves. RFs are typically contaminated by the "scattered" wave field, the portion of the *P*−wave coda that arises from multiple scattering and conversion in a strongly heterogeneous crust (Abers, 1998). In this study we apply a new RF−estimation technique (Park and Levin, 2000a) that uses multiple−taper spectral correlation estimates (Vernon et al 1991) instead of spectral ratios.

The multitaper RF algorithm has two distinct advantages. First, it estimates the receiver functions $H_R(f)$ and $H_T(f)$ only from the portion of the horizontal motion that is correlated (in a narrow frequency band) with the vertical motion. Second, the relative proportion of uncorrelated horizontal motion, as quantified by the spectral coherences $C_R(f)$ and $C_T(f)$, is used to estimate the uncertainty of $H_R(f)$ and $H_T(f)$. (High coherence

implies low uncertainty.) These uncertainties can be used to weight RF−estimates from different earthquakes when estimating a composite, or "stacked," receiver function in the frequency domain. There is no formal uncertainty estimate for the time−domain multitaper RF, but an informal assessment can be made from the acausal part of the RF i.e. the amplitude of $H_R(t)$, $H_T(t)$ for $t<0$. In our experience with real data, the coherence between horizontal and vertical motion in a P coda is highly frequency dependent, and the pattern of frequency dependence can vary greatly from event to event. Therefore the use of uncertainty−based weights in multiple−record RF estimation is important. With stacking, much higher−frequency RFs can be resolved (Figure 1), well over $f=1$ Hz. For geologic applications, this allows much finer depth resolution to determine e.g., the thickness of the Moho transition. For CTBT monitoring, this allows us to characterize deterministic seismic scattering at frequencies of nonproliferation interest.

We have applied our new RF technique to GSN station PET (Petropavlovsk−Kamchatsky, Russia), ARU (Arti, Russia), YSS (Yuzhno−Sakhalinsk, Russia, ADK (Adak, Alaska), MAJO (Matsushiro, Japan), COL (College, Alaska) and COR (Corvallis, Oregon) (Park and Levin, 2000a; Yuan et al 1999). We have focussed particularly on data recorded at two important GSN stations in the Middle East, RAYN (Ar Rayn, Saudi, Arabia) and ANTO (Ankara, Turkey) (Levin and Park 2000; Park and Levin 2000b; see Figure 2).

Shear zones in the Proterozoic lithosphere of the Arabian Shield and the nature of the Hales discontinuity.

Seismic velocity discontinuities are commonly found within the upper 100 km of the mantle lithosphere, with great variability in their depth, lateral extent, and the polarity of velocity jump. Among the more commonly observed is the "80 km" or Hales discontinuity, identified in a variety of tectonic environments (Hales, 1969; Pavlenkova, 1996; Bostock, 1997), and sometimes associated with seismic anisotropy. Anisotropy is associated with the crust−mantle transition, and with another anomalous region ~70 km deep, which we interpret as containing the Hales discontinuity. Azimuthal patterns and frequency dependence of pulse shapes of observed *P−SH* converted waves (Figure 3) suggest that both zones are bound by discontinuities in anisotropic properties on one side, and by smooth gradients on another. In our preferred model anisotropic zones extend downward from the Moho and the Hales discontinuities (Figure 4). Within both zones the anisotropic symmetry axes, indicative of systematic fabric in the olivine−dominated upper mantle material, are oriented along the N−S direction (±10°), and are tilted 50° to the south.

We interpret our findings as evidence for thin shear zones within the mantle lithosphere, developed after the assembly of the Arabian Shield during a late Proterozoic continent−continent collision (Figure 5). Post−collisional tectonics created the Najd fault system and involved the Ar−Rayn block in an "escape tectonics" episode along the trajectory that would be close to present−day N−S direction. Preservation of these shear zones for ~500 My within the upper mantle is in good agreement with geochemical evidence for common tectonic history of the crust and upper mantle composing the Arabian Shield.

Although recognised globally, the details of the Hales discontinuity appear to be tied to the tectonic history of a specific location (Arabian shield, Slave craton). Therefore, a single origin of this seismic feature, analogous to the mineral phase changes at 420− and 670−km depth, may be hard to constrain. Rather, we hypothesize that the typical depth range of the Hales discontinuity (60−90 km) is where tectonic events often leave their "marks" in the continental lithosphere, perhaps indicating the minimum thickness of the stiff mantle lid in orogenic events. Proterozoic stretch marks from similar dynamics may be preserved within the shallow lithosphere of the Arabian Shield. The receiver function study of Sandvol et al. (1998a) suggests a variable depth to an interface in the Hales depth range across the southeastern portion of the Shield, but does not analyze the transverse component. Our experience with RAYN, for which Sandvol et al. (1998a) reported no P_{Hs} phase, suggests that the azimuthal dependence of the transverse RF is a crucial constraint on the relict strains embedded within continental lithosphere.

Receiver Functions From Near−Teleseismic and Regional P Waves.

The extended codas of regional P waves, suggestive of intense scattering, discourage their analysis with traditional receiver−function (RF) estimation algorithms. However, reflectivity seismograms using a locked mode approximation demonstrate that the extended nature of regional *P* can be simulated with a 1−D model, for which off−path− and back−scattering is absent (Park and Levin, 2000b). Complex scattering is surely present in real data from regional distances, but spectral cross−correlation mitigates its influence on receiver−function estimation. Using multiple−taper spectral cross−correlation, stable receiver functions (RFs) can be estimated from regional and near−teleseismic *P* waves (Park and Levin, 2000b). Resolution of *Ps* converted energy is greatly improved by averaging single−event RFs in the frequency domain in narrow epicentral−distance bins.

Stations RAYN and ANTO represent, to some extent, the extremes of what one might expect in receiver−function studies. RAYN lies atop a stable shield with minimal sediment cover, and primary *Ps* conversions from the Moho are readily retrievable from reverbatory shallow−incidence regional and near−teleseismic *P* waves (Figure 6). Although sited on hard rock, ANTO lies within a river valley in an actively deforming region, close to the active North Anatolian fault system. For events from the east to ANTO, the *Ps* conversions at f>1 Hz appear to be strongly influenced by shallow 3−D structures (Figure 7). In particular, some negative pulses in the RFs move out to shorter delays as Δ−−>0, a behavior we find easiest to model with *P*−*P* and *P*−*S* scattering from a surface or near−surface obstacle 20−30 km eastward of ANTO (Figure 8). For events from the west to ANTO, Moho−converted *Ps* energy is easier to identify in the regional RFs. For both stations the radial RFs estimated from regional *P* agree well with the radial RFs from teleseismic *P*. This implies that some features in the teleseismic receiver functions for ANTO, as estimated from eastern backazimuths, may actually represent topographic scattering rather than *Ps* conversions from deep crustal and mantle interfaces. We conclude that receiver functions from regional *P* are useful to check the suitability of teleseismic receiver functions for 1−D structure inversion.

A strong east−west asymmetry in the ANTO regional−*P* receiver functions is consistent with previous observations of regional−wave propagation. Rodgers et al. (1997) and Gok et al. (2000) report inefficient S_n and *Lg* propagation for regional−distance events from the east and southeast to ANTO, and efficient propagation from the west. East of ANTO lie the Turkish and Iranian plateaus, characterized by Cong and Mitchell (1998) as having depressed shear velocities and high attenuation (Q<100 in the crust). Regional waves from the east traverse a continental collisional zone extending from central Anatolia through the Zagros mountains in southwest Iran. Broadband stations GNI (Garni, Armenia) and TBZ (Trabzon, Turkey) lie within this collision zone in eastern Anatolia. Sandvol et al. (1998b) and Cakir et al. (2000), report complex receiver functions for, respectively, GNI and TBZ, and derive models from the radial RFs with low−velocity zones in the shallow mantle. If low velocities and low Q imply subsolidus temperatures and partial melt, as suggested by Cong and Mitchell (1998) and Cakir et al. (2000), the propagation of regional phases would likely be disrupted.

Regional RFs for RAYN and for western backazimuths at ANTO show complexity in the inferred Moho *Ps* phase near Δ=20°. This appears to be consistent with (1) the triplication of *P* associated with velocity gradients in the mantle transition zone, and (2) a merging of teleseismic and regional *P*, both of which imply overlapping phases with distinct incidence angles and (therefore) distinct Ps delay times relative to direct *P*. Many of the general features of regional *P* receiver functions are confirmed with receiver functions estimated from synthetic seismograms, computed using a locked−mode approximation with a anisotropic reflectivity code. The reverberative nature of P_n and P_g phases leads to complex radial RFs with small "acausal" pulses and a train of causal pulses whose amplitude varies strongly with epicentral distance and with the details of crustal structure, all in the absence of lateral structure. Using a simple reflectivity code with an upgoing plane−wave predicts significant *P*−to−*SH* conversion at the Moho at near−horizontal incidence, but locked−mode synthetics suggest that regional−*P*−to−*SH* conversion is very weak for modest levels of anisotropy. In the context of 1−D models, it appears possible to generate nonnegligible transverse motion in regional *P* with shallow, but not anisotropy near the Moho. However, *P*−to−*SH* conversion is not as large in our synthetics as would appear to be the case in data from RAYN and ANTO. Either shallow crustal anisotropy is much larger than ~5% or else scattering from 2−D and 3−D structures is pervasive in the observed phases.

CONCLUSIONS AND RECOMMENDATIONS

A significant proportion of the scattered wave field, even at *f>1* Hz, appears to be characterized by a predictable series of *P*−to−*S* conversions by horizontal or near−horizontal interfaces in the crust and shallow mantle. These converted phases typically have polarity changes with back−azimuth that are consistent with elastic anisotropy as the cause of *P*−to−*S* scattering. Our investigations suggest that the continental mantle, in some locales, possesses thin layers (10−20 km) of sheared rock, from past tectonic events, that cause *P*−to−*S* scattering.

Not all scattering can be predicted by a receiver function, of course. Often a large proportion of the scattered wave field on the horizontal components is incoherent with the vertical component. Poor coherence biases normal RF estimators, but is alleviated by the new multiple−taper receiver−function estimator we have developed.

We recommend continued use of back−azimuth and range−dependent receiver functions to characterize scattering at broadband seismic monitoring stations within the verification system of the CTBT. Data analysis from our preliminary suite of stations suggests that a 1−D anisotropic crustal structure is appropriate

for modeling a significant portion of crustal scattering in teleseismic signals. Receiver function analysis is applicable to regional and near−teleseismic *P* in some cases (RAYN and ANTO from the west, but not ANTO from the east). This suggests that new methods to characterize regional−distance scattering empirically may be fruitful. Further work should focus on data from other continental regions. Application of multiple−taper coherence methods to the study of scattered waves in seismic array data should be pursued.

REFERENCES

Abers, G. A., Array measurements of phases used in receiver−function calculations; importance of scattering. **Bull. Seism. Soc. Amer., 87**, 313−318, 1998.

Babuska, V., and Cara, M., **Seismic Anisotropy in the Earth**, Kluwer Academic, Dordrecht, 1991.

Bostock, M. G., Anisotropic upper−mantle stratigraphy and architecture of the Slave craton, **Nature, 390**, 393−395, 1997.

Cakir, O., Erduran, M., Cinar, H., and Yilmazturk, A., Forward modelling receiver functions for crustal structure beneath station TBZ (Trabzon, Turkey), **Geophys. J. Int., 140**, 341−356, 2000.

Cassidy, J. F., Numerical experiments in broadband receiver function analysis, **Bull. Seism. Soc. Amer., 82**, 1453−1474, 1992.

Cong, L., and Mitchell, B. J., Seismic velocity and Q structure of the Middle Eastern crust and upper mantle from surface wave dispersion and attenuation, **Pure Appl. Geophys., 153**, 503−538, 1998.

Gok, R., Turkelli, N., Sandvol, E., Seber, D. and Barazangi, M., Regional wave propagation in Turkey and surrounding regions, **Geophys. Res. Letts. 27**, 429−432, 2000.

Helbig, K., **Foundations of Anisotropy for Exploration Seismics**, Pergammon/Elsevier Science, Oxford, 1994.

Hudson, J. A., Wave speeds and attenuation of elastic waves in material containing cracks, **Geophys. J. Roy. Astron. Soc., 64**, 133−150, 1981.

Kosarev, G. L., Makeyeva, L. I. and Vinnik, L. P., Anisotropy of the mantle inferred from observations of P to S converted waves, **Geophys. J. Roy. Astron. Soc., 76**, 209−220, 1984.

Levander, A. R., and Hollinger, K., Small−scale heterogeneity and large−scale velocity structure of the continental crust, **J. Geophys. Res., 97,** 8797−8804, 1992.

Hales, A. L., A seismic discontinuity in the lithosphere. **Earth Planet. Sci. Letts., 7**, 44−46, 1969.

Levin, V., and J. Park, P−SH conversions in a flat−layered medium with anisotropy of arbitrary orientation, **Geophys. J. Int., 131**, 253−266, 1997.

Levin, V., and J. Park, A P−SH conversion in layered media with hexagonally symmetric anisotropy: A cookbook, **Pure and Applied Geophysics, 151**, 669−697, 1998.

Levin, V. and Park, J., Shear zones in the Proterozoic lithosphere of the Arabian Shield and the nature of the Hales discontinuity, **Tectonophysics**, in press, 2000.

Park, J., Surface waves in layered anisotropic structures, **Geophys. J. Int., 126**, 173−184, 1996.

Park, J. and Levin, V., Receiver functions from multiple−taper spectral correlation estimates, **Bull. Seism. Soc. Amer.**, submitted 2000a.

Park, J. and Levin, V., Receiver functions From regional P waves, **Geophys. J. Int.**, submitted 2000b.

Pavlenkova, N. I., General features of the uppermost mantle stratification from long−range seismic profiles. **Tectonophysics**, 264, 261−278, 1996.

Rodgers, A. J., Ni, J. F., Hearn, T. M., Propagation characteristics of short−period Sn and Lg in the Middle East, **Bull. Seism. Soc. Amer., 87**, 396−413, 1997.

Sandvol, E., Seber, D., Barazangi, M., Vernon, F. L., Mellors, R., and Al−Amri, A., Lithospheric seismic velocity discontinuities beneath the Arabian Shield. **Geophys. Res. Letts., 25**, 2873−2876, 1998a.

Sandvol, E., Seber, D., Calvert, A., and Barazangi, M., Grid search modeling of receiver functions; i crustal structure in the Middle East and North Africa, **J. Geophys. Res., 103**, 26899−26917, 1998b.

Savage, M., Lower crustal anisotropy or dipping boundaries? Effects on receiver functions and a case study in New Zealand, **J. Geophys. Res., 103**, 15069−15087, 1998.

Vernon, F. L., J. Fletcher, L. Carroll, A. Chave and E. Sembrera, Coherence of seismic body waves from local events as measured by a small−aperture array, **J. Geophys. Res., 96,** 11981−11996, 1991.

Wu, R.−S., Wide−angle elastic wave one−way propagation in heterogeneous media and an elastic wave complex screen method, **J. Geophys. Res., 99**, 751−766, 1994.

Yuan, H., J. Park and V. Levin, P−to−S converted phases from subducted slabs in the Northwest Pacific, **EOS Trans. AGU**, Fall Supplement, 80, F720, 1999.

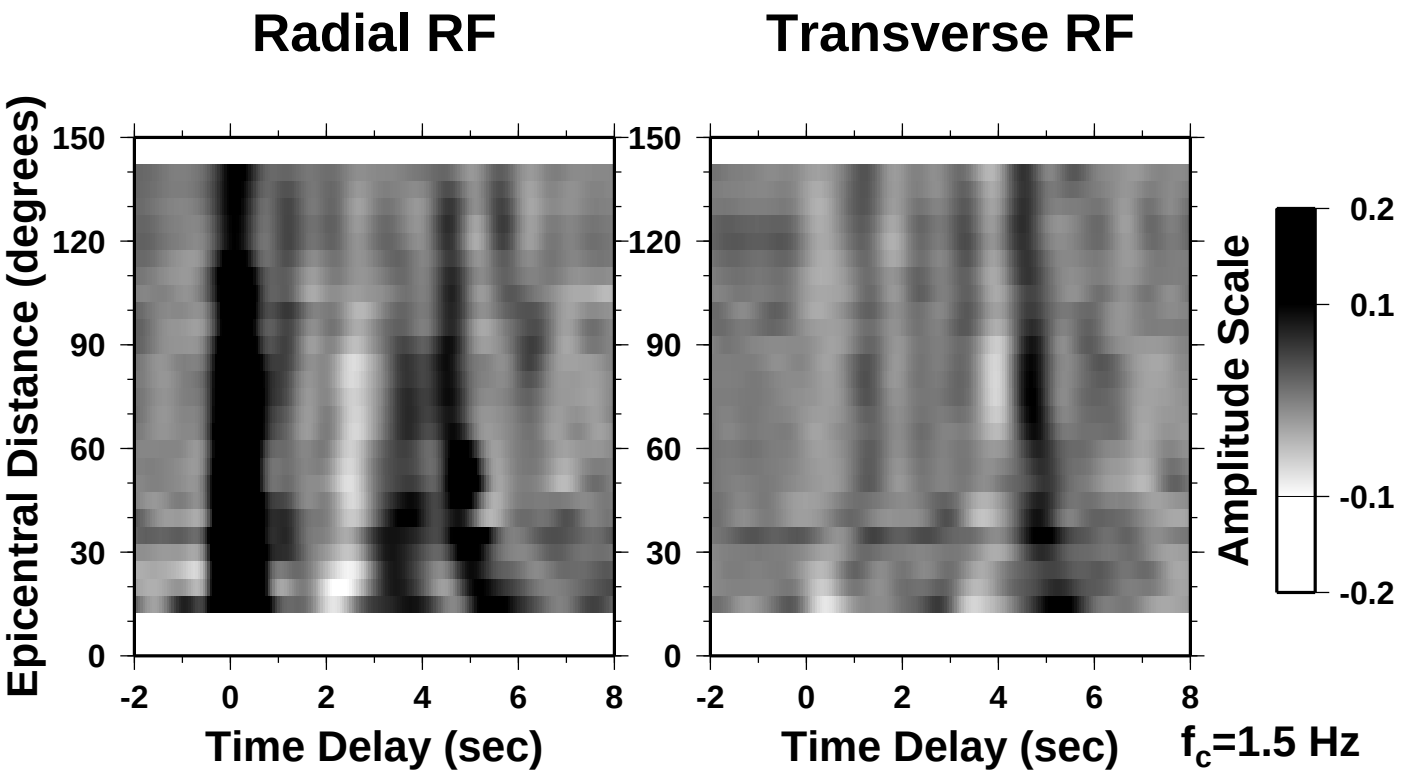

Figure 1. Grey-shade plots of composite receiver-functions at ARU (Arti, Russia) for frequency cutoffs f_c=1.5 Hz (above) and f_c=6.0 Hz (below), plotted against epicentral distance Δ. Only events in the back-azimuth range 50˚-150˚ contribute to the composite RFs. Over 200 P-coda are stacked in the images.

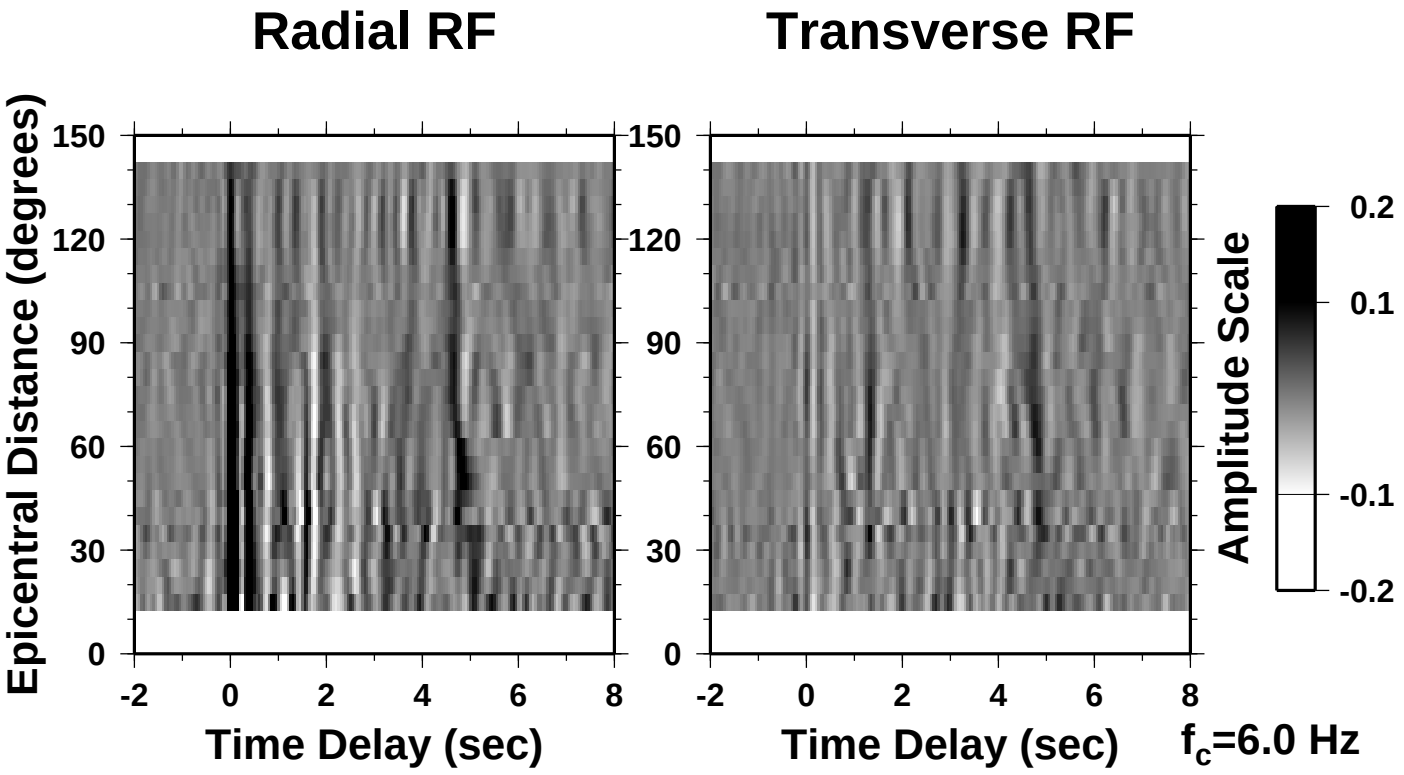

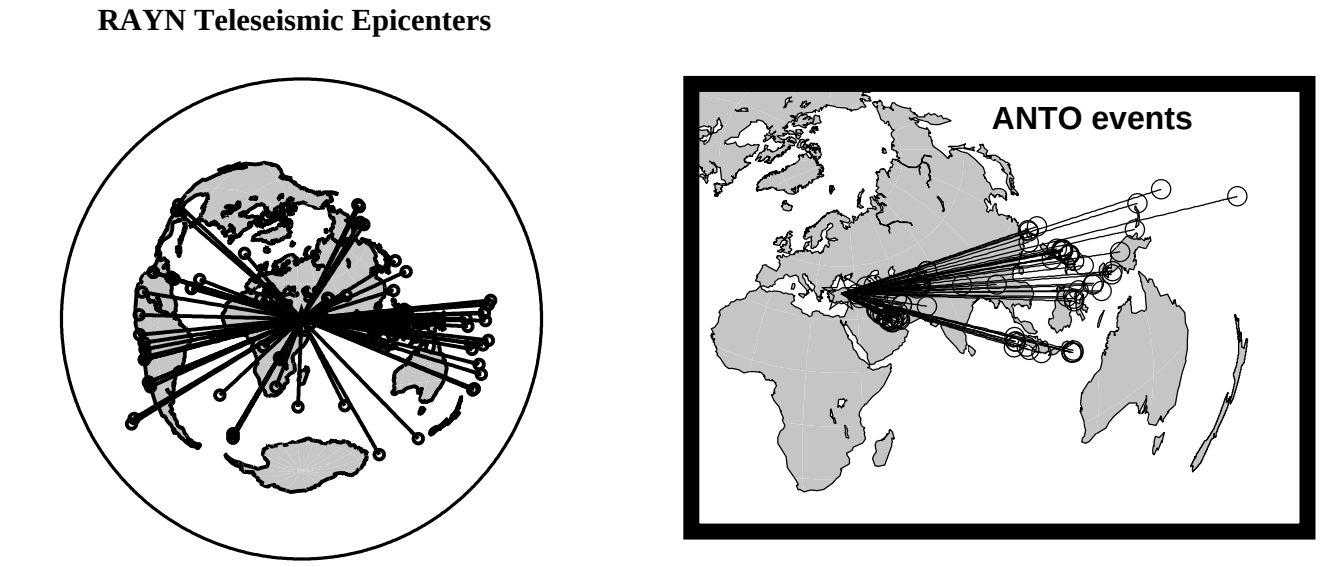

Figure 2. Events for Middle East stations. Regional earthquakes are analyzed in a narrow back-azimuth sector.

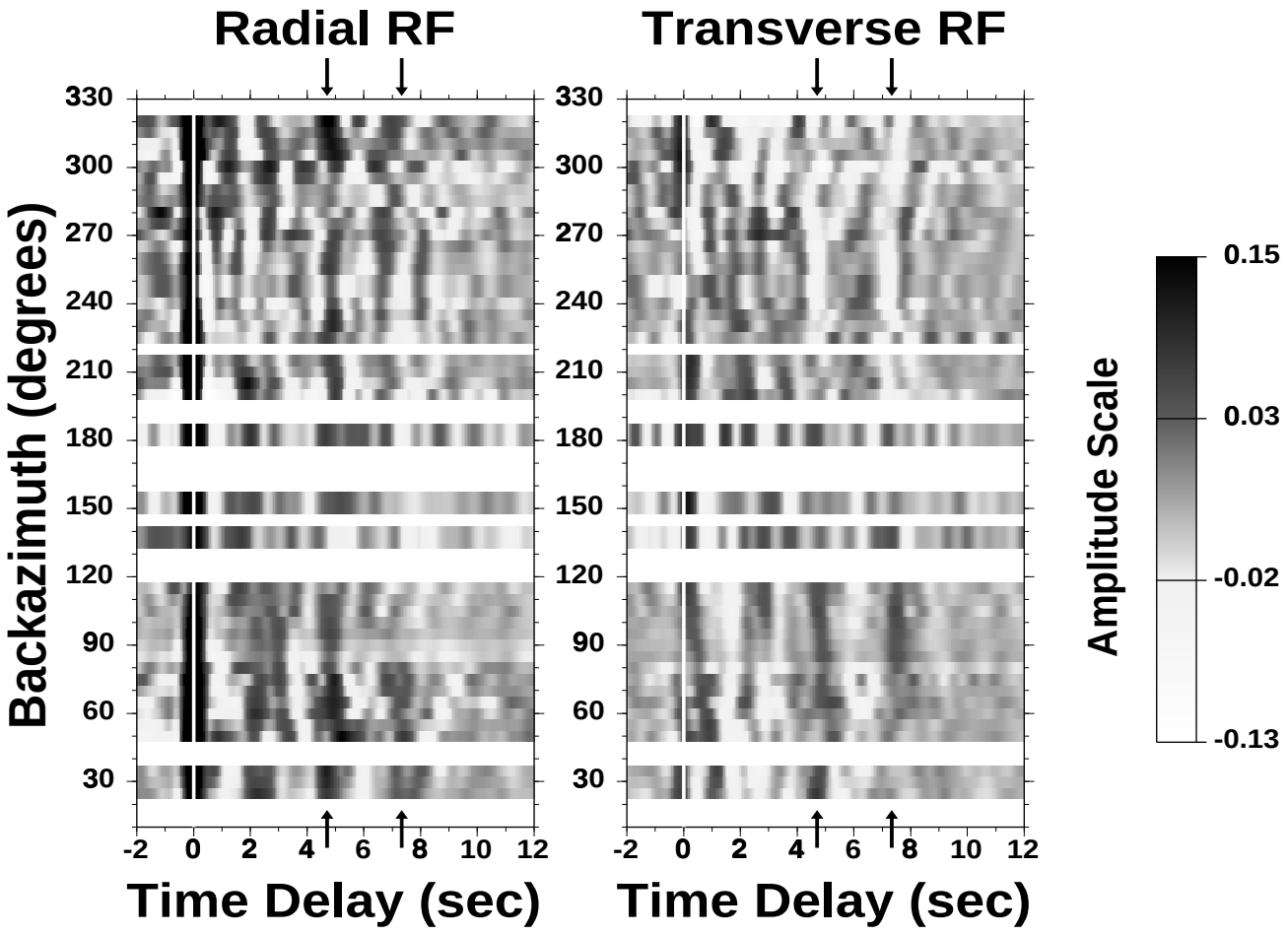

Figure 3. RAYN receiver functions as a function of back-azimuth. Data include direct P, PKP, and Pdiff phases observed between spring 1997 and summer 1999. RF spectra are lowpassed (effectively) at 1 Hz (fc=2.0 Hz). The converted phases Pms and PHs are indicated by arrows at roughly 4.8 and 7.2-sec delay. Note the polarity changes in the transverse RFs for these phases. Conversions from the east have positive amplitude, conversions from the west are negative.

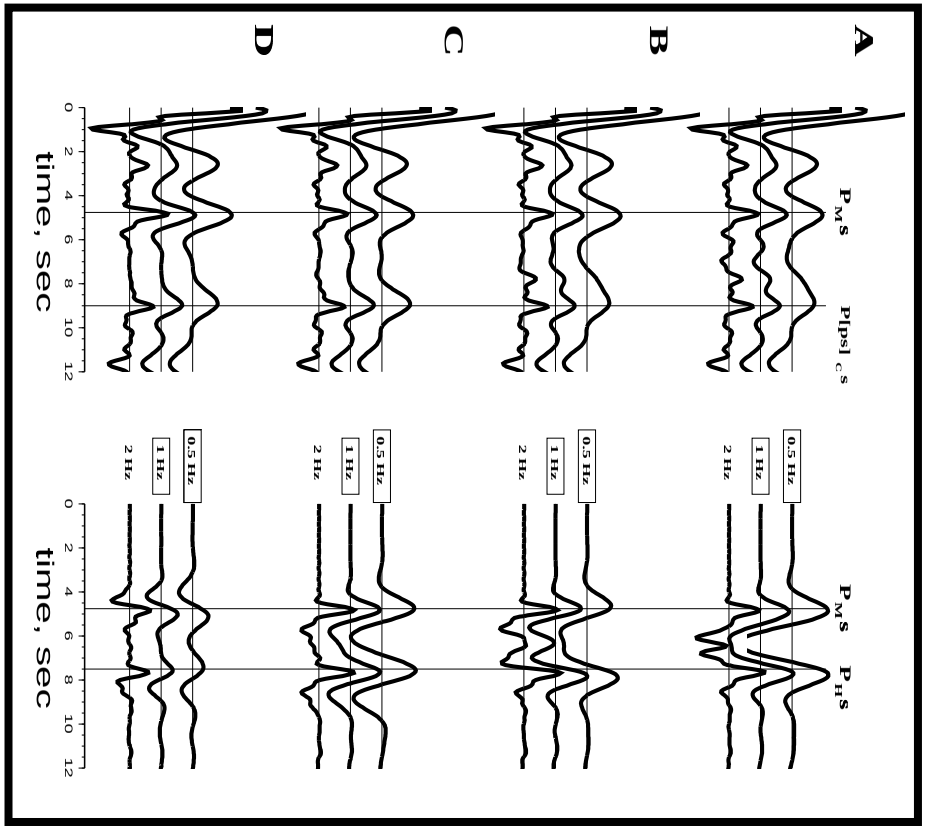

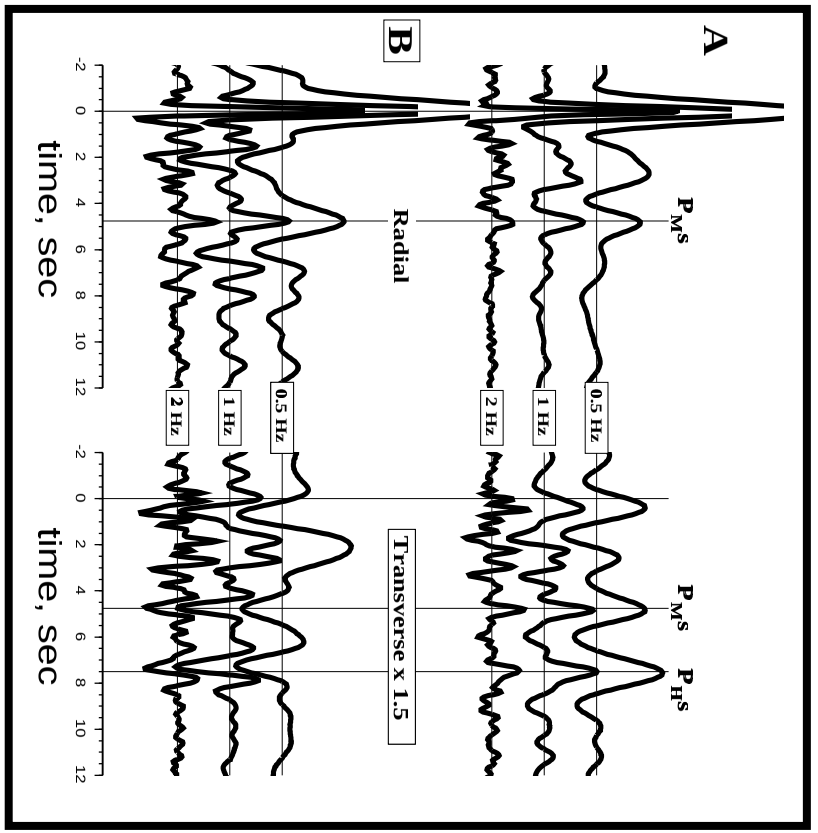

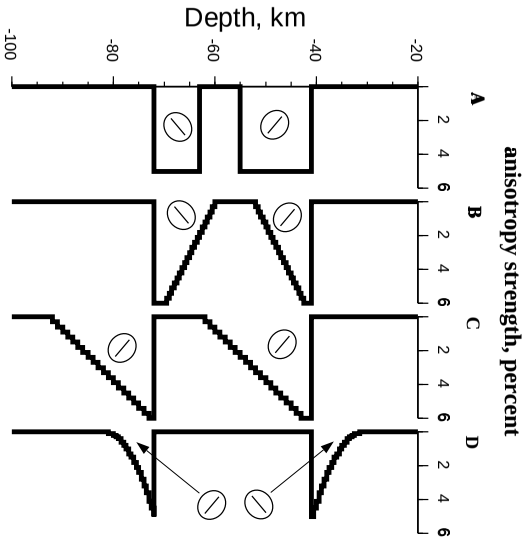

Figure 4. Upper Left: Composite RAYN RFs for narrow backazimuthal ranges for a variety of cutoff frequencies. The eastern stack (A) includes data from backazimuths 75°–107°; The western stack (B) includes data from backazimths 255°–285°. P_Ms is clear in all frequencies on both radial and transverse components, while P_Hs is primarily seen on the transverse component. Time-alignment of P_Hs is better at high frequencies. Lower Right: Vertical profiles of anisotropy strength in the models we tested for RAYN RFs. Coffee-bean symbols show the orientation of symmetry axis of anisotropy. Symmetry-axis tilt (from the vertical) toward the south is indicated by a symbol that tips to the left. Lower Left: Synthetic RFs for a P wave incident from the east. The 2-Hz receiver functions for Model C provide the best match to the one-sided pulses on the RAYN RFs from eastern backazimuths. Model D, with a slightly different anisotropic gradient beneath the Hales discontinuity, matches better the P_Hs pulse from western backazimuths.

Figure 5. Schematic diagram illustrating the development of shear zones within the upper mantle beneath the Ar Rayn terrane of the Arabian Shield, during an episode of northward "tectonic escape" in the late Proterozoic. Arrows beneath the Moho and Hales discontinuities indicate the location and direction of lattice-preferred orientation in olivine grains suggested by Model C.

Figure 6. Regional and near-teleseismic RAYN receiver functions, averaged in 4° epicentral-distance bins in the frequency domains with uncertainty handicaps. Results for short-period data (40 sps) are shown for eastern backazimuths, with frequency cutoff $f = 10$ Hz. Superimposed delay curves are computed for the Ps converted phases that would arise from a Moho at 41 km depth for incoming P and P_n waves using the phase velocities of the IASPEI91 model.

6

Figure 7. ANTO receiver functions, averaged in 10° epicentral-distance bins in the frequency domains with uncertainty handicaps. Results for events from eastern backazimuths are shown, with frequency cutoff $f = 3$ Hz. The thin solid lines indicate predicted Ps arrival delays computed from the RAYN crustal model, from a midcrustal interface, the Moho and a hypothetical Hale discontinuity. The RF traces are shaded on the negative side to highlight features whose delays decrease as $\Delta \to 0$. Note the continuity of RF pulses from teleseismic to regional distances, especially at short delay times.

7

Figure 8. Moveout curves for simple scenarios of Ps scattering, using an upgoing plane-wave slowness from the IASPEI91 earth model. The Moho depth is taken to be 40 km beneath a hypothetical station, and crustal V_P and V_S are 6.0 and $6/\sqrt{3}$, respectively. The mantle V_P is 8.0 km/sec. Curve "FM" indicates Ps delays for a flat Moho. Curve "DM" indicates Ps delays for a Moho that dips 40°, with direct-P approaching from the updip side. Curves "S" and "SS" in the left panel indicate P_{DS} and Ps_{DS} phases that convert and reflect, respectively, from a shallow interface D. Curves "SP" and "SS" in the right panel indicate the arrivals of P and S waves, respectively, from a surface scatterer 30 km from the station, between source and receiver. Only the surface scatterer causes negative moveout as $\Delta \to 0$ similar to ANTO RF features in Figure 7.